

THERMODYNAMIC AND KINETIC INVESTIGATIONS OF HEXYLAMINE AS A  
CORROSION INHIBITOR FOR CARBON STEEL IN HYDROCHLORIC ACID MEDIABoshra Ahmed Abazid\*<sup>1</sup><sup>1</sup>Department of Chemistry Homs University, Homs, Syria.

Article Received: 01 May 2026

Article Revised: 22 May 2026

Article Published: 01 June 2026



\*Corresponding Author: Boshra Ahmed Abazid

Department of Chemistry Homs University, Homs, Syria.

DOI: <https://doi.org/10.5281/zenodo.20444101>**How to cite this Article:** Boshra Ahmed Abazid\*<sup>1</sup> (2026). Thermodynamic And Kinetic Investigations Of Hexylamine As A Corrosion Inhibitor For Carbon Steel In Hydrochloric Acid Media. World Journal of Advance Healthcare Research, 10(6), 105–112.

This work is licensed under Creative Commons Attribution 4.0 International license.

## ABSTRACT

The electrochemical degradation of carbon steel in acidic media constitutes a significant industrial challenge, necessitating the development of efficient and structurally optimized corrosion inhibitors. This study evaluates the inhibitory efficacy of hexylamine (HA) on carbon steel in 0.1 M hydrochloric acid employing gravimetric measurements across a controlled temperature range of 298–308 K. Inhibition efficiency (IE%) exhibited a direct concentration dependence, attaining a maximum value of 94.9% at 0.025 M and 298 K, while demonstrating a marginal decline with increasing temperature due to partial thermal desorption of the adsorbed film. The interfacial adsorption process conformed precisely to the Langmuir isotherm model at all investigated temperatures, confirming monolayer coverage without significant lateral interactions. Kinetic analysis revealed a systematic increase in apparent activation energy ( $E_a$ ) and enthalpy of activation ( $\Delta H_a$ ) in the presence of HA, indicative of an elevated energy barrier for anodic metal dissolution and an endothermic corrosion process. Thermodynamic evaluation yielded standard Gibbs free energy of adsorption ( $\Delta G_{ads}^\circ$ ) values ranging from  $-24.20$  to  $-24.64$  kJ·mol<sup>-1</sup>, signifying a spontaneous adsorption process governed by a mixed physisorption–chemisorption mechanism. Furthermore, the enthalpy of adsorption and entropy of adsorption were mechanistically rationalized through a quasi-substitution model, wherein the displacement of multiple pre-adsorbed water molecules by a single hexylamine molecule result in a net increase in interfacial disorder. These findings establish hexylamine as a highly effective, thermodynamically stable inhibitor for mitigating acid-induced corrosion in industrial pickling applications.

**KEYWORDS:** Hexylamine, Carbon steel corrosion, Hydrochloric acid, Corrosion inhibition, Langmuir adsorption isotherm, Thermodynamic parameters, Quasi-substitution mechanism.

## 1. INTRODUCTION

The electrochemical degradation of metallic infrastructure represents a pervasive and economically consequential challenge across industrial sectors, with global annual expenditures attributed to corrosion consistently estimated at 3.5–5% of national gross domestic products.<sup>[1,2]</sup> In aggressive acidic environments, particularly hydrochloric acid (HCl) media routinely employed in acid pickling, descaling operations, and petroleum well-stimulation, the accelerated anodic dissolution of ferrous and non-ferrous alloys necessitates the implementation of robust mitigation strategies.<sup>[3,4]</sup> Among the diverse methodologies deployed for

corrosion control, the application of organic corrosion inhibitors has emerged as one of the most technically effective and economically viable approaches, owing to their molecular tunability and capacity for targeted surface interaction.<sup>[5]</sup>

The inhibitory efficacy of organic compounds is fundamentally governed by their electronic architecture and physicochemical properties. Inhibition typically proceeds via the adsorption of inhibitor molecules onto the metallic substrate, wherein heteroatoms possessing non-bonding electron pairs (e.g., N, O, S, P) facilitate coordinate bonding with vacant d-orbitals of surface

metal atoms.<sup>[2,6]</sup> This adsorption phenomenon, which may manifest as physisorption, chemisorption, or a synergistic physiochemisorption mechanism, culminates in the formation of a compact interfacial barrier that impedes the diffusion of corrosive species to the metal–electrolyte boundary.<sup>[7,8]</sup> Contemporary structure–activity analyses consistently demonstrate that molecular planarity, extended  $\pi$ -conjugation, and the presence of electron-donating substituents markedly enhance surface coverage and strengthen metal–inhibitor interactions, thereby elevating protection efficiency.<sup>[9-12]</sup>

Within the expansive catalog of organic inhibitors, amine derivatives have garnered substantial scientific interest due to their versatile coordination chemistry and adaptable hydrophobic–hydrophilic equilibrium. Aliphatic primary (1°), secondary (2°), and tertiary (3°) amines function as potent corrosion inhibitors by anchoring to the metallic surface through the polar amine moiety, while the appended alkyl chains confer hydrophobic character that repels aqueous corrosive media.<sup>[13-16]</sup> A well-documented structure–property relationship indicates that inhibition efficiency generally correlates positively with the elongation of the aliphatic chain, as extended hydrophobic domains enhance barrier integrity; however, excessive chain extension frequently compromises aqueous solubility, particularly in polar electrolytic systems, thereby diminishing practical applicability.<sup>[14-17]</sup> Consequently, the rational design of amine-based inhibitors necessitates an optimal thermodynamic and solvation balance between hydrophilic adsorption centers and hydrophobic protective tails.<sup>[2,16]</sup>

Hexylamine (C<sub>6</sub>H<sub>15</sub>N), a primary aliphatic amine characterized by a linear six-carbon alkyl chain, represents a strategically relevant candidate for corrosion mitigation in HCl environments. Preliminary investigations on homologous aliphatic amines demonstrate that compounds within the C<sub>6</sub>–C<sub>12</sub> range exhibit pronounced mixed-type inhibition behavior, predominantly adhering to the Langmuir adsorption isotherm model while significantly modulating both anodic metal dissolution and cathodic hydrogen evolution kinetics.<sup>[16,17]</sup> Despite these foundational insights, a comprehensive elucidation of hexylamine's adsorption thermodynamics, interfacial charge-transfer resistance, and molecular-level interaction mechanisms in aggressive chloride media remains requisite for the optimization of green, high-performance inhibitor formulations.

The purpose of the present work is to investigate the effect of Hexylamine (HA) as corrosion inhibitor for carbon steel in 1M HCl at various temperatures using gravimetric measurements. The kinetic and adsorption parameters of corrosion inhibition process are also evaluated and discussed.

## 2. Experimental

### 2.1. Materials And Apparatus

Hexylamine (HA), the steel used in this study is a carbon steel (ST37) with a chemical composition (in wt%) of 0.08 % C, 0.05 % S, 0.25 % Mn, 0.04 % P, and the remainder iron (Fe). The carbon steel samples were pre-treated prior to the experiments by grinding with emery paper SiC (80, 180, 400, 600 and 1200); rinsed with distilled water, again with bi distilled water and then dried at room temperature before use. The acid solutions (0.1 M HCl) were prepared by dilution of an analytical reagent grade 37 % HCl with double-distilled water. The concentration range of Hexylamine (HA) employed was 0.01-0.025 M.

### 2.2. Weight loss measurements

Mild steel coupons with precise dimensions of 4.2 cm × 2.0 cm × 0.1 cm were subjected to sequential mechanical abrasion using silicon carbide emery papers of progressively finer grades (ranging from 180 to 1200 grit) to ensure a reproducible and homogeneous surface finish. Following abrasion, the specimens were thoroughly rinsed with double-distilled water to remove particulate debris, subsequently degreased via ultrasonic cleaning in analytical-grade acetone, and finally dried under a stream of high-purity nitrogen gas. The prepared coupons were then stored in a vacuum desiccator containing anhydrous calcium sulfate to prevent atmospheric contamination prior to experimental deployment.

Initial masses of the specimens were determined using a calibrated analytical balance with a readability of ±0.01 mg. Subsequently, each coupon was fully immersed in 100 mL of aerated 0.1 M hydrochloric acid (HCl) test solution, both in the absence and presence of varying concentrations of the investigated corrosion inhibitor (hexylamine). All immersion tests were conducted under static conditions at ambient temperature (25-35 ± 1 °C) for a standardized duration of 6 hours to ensure comparability across experimental runs. Upon completion of the exposure period, the specimens were carefully withdrawn, gently rinsed with absolute ethanol to eliminate residual electrolyte and loosely adherent corrosion products, dried as previously described, and re-weighed to determine mass loss attributable to corrosive dissolution.

The mean corrosion rate (CR), expressed in milligrams per square centimeter per hour (mg·cm<sup>-2</sup>·h<sup>-1</sup>), was computed according to Equation (1). The inhibition efficiency (IE%), reflecting the protective capacity of hexylamine, was subsequently derived using Equation (2).

$$CR = \frac{w_0 - w}{A.t} \quad (1)$$

$$IE\% = \frac{CR_0 - CR}{CR_0} * 100 \quad (2)$$

The degree of surface coverage for different concentrations of inhibitor is calculated using

$$\theta = \frac{CR_0 - CR}{CR_0} = \frac{IE\%}{100} \quad (3)$$

where  $w_0$  and  $w$  are the weights of carbon steel sheet before and after experiments  $A$  is the total surface area of the specimen,  $t$  is the immersion time and  $CR_0$  and  $CR$  are values of the corrosion rate without and with addition of the inhibitor, respectively.

### 3. RESULTS AND DISCUSSION

#### 3.1. Effect of temperature and kinetic parameters of activation

The gravimetric data presented in Table 1 delineate the temperature-dependent corrosion behaviour of carbon steel in 0.1 M hydrochloric acid in the absence and presence of varying concentrations of hexylamine (HA). A systematic analysis reveals two concurrent trends: (i) at constant inhibitor concentration, the corrosion rate (CR) exhibits a positive correlation with temperature, increasing from 2.3148  $\text{mg}\cdot\text{cm}^{-2}\cdot\text{h}^{-1}$  at 298 K to 4.6417  $\text{mg}\cdot\text{cm}^{-2}\cdot\text{h}^{-1}$  at 308 K for the uninhibited system; and (ii) at constant temperature, CR demonstrates an inverse relationship with HA concentration, decreasing to 0.1703  $\text{mg}\cdot\text{cm}^{-2}\cdot\text{h}^{-1}$  at 0.025 M and 298 K. Correspondingly, inhibition efficiency (IE%) attains a maximum value of 94.9% under these conditions, consistent with enhanced surface coverage ( $\theta$ ) and the establishment of a more cohesive interfacial barrier.<sup>[18, 19]</sup>

The observed acceleration of corrosive dissolution with increasing temperature is attributable to the enhanced kinetic energy of aggressive chloride ions and the thermally induced destabilisation of the adsorbed inhibitor film.<sup>[10, 20]</sup>

To elucidate the energetics governing the corrosion process, the apparent activation energy ( $E_a$ ) was derived from the linearised Arrhenius equation (Equation 4).<sup>[21]</sup>

$$CR = A \exp\left(\frac{-E_a}{RT}\right), \quad \ln(CR) = \ln A - \frac{E_a}{RT} \quad (4)$$

where  $E_a$  represents the apparent activation energy,  $R$  is the molar gas constant ( $8.31434 \text{ J}\cdot\text{K}^{-1}\cdot\text{mol}^{-1}$ ), and  $A$  represents the pre-exponential factor. Arrhenius plots for

the corrosion rate of carbon steel are given in Figure 1. Values of  $E_a$  for carbon steel corrosion in 0.1 M HCl in the absence and presence of (HA) were calculated by linear regression between  $\ln(CR)$  and  $1/T$  and are listed in Table 2. An alternative form of Arrhenius equation is also used to calculate enthalpy and entropy of activation.

$$CR = \frac{RT}{Nh} \exp\left(\frac{\Delta S_a}{R}\right) \exp\left(\frac{-\Delta H_a}{RT}\right) \quad (5)$$

$$\ln\left(\frac{CR}{T}\right) = \ln\left(\frac{R}{Nh}\right) + \frac{\Delta S_a}{R} - \frac{-\Delta H_a}{RT}$$

where  $CR$  is the corrosion rate,  $h$  is the Planck's constant ( $6.626176 \times 10^{-34} \text{ Js}$ ),  $N$  is the Avogadro's number ( $6.02252 \times 10^{23} \text{ mol}^{-1}$ ),  $R$  is the universal gas constant and  $T$  is the absolute temperature,  $\Delta H_a$  the enthalpy of activation, and  $\Delta S_a$  entropy of activation. The values of enthalpy of activation  $\Delta H_a$  and entropy of activation,  $\Delta S_a$  were obtained from the transition state equation (5). A plot of  $\ln(CR/T)$  as a function of  $1/T$  (Fig. 2) was made for carbon steel corrosion in 0.1 M HCl in the absence and presence of different concentrations of (HA). Straight lines are obtained with a slope ( $-\Delta H_a/R$ ) and intercept ( $\ln(R/Nh) + \Delta S_a/R$ ) from which the  $\Delta H_a$  and  $\Delta S_a$  values are calculated (Table 2).

**Table 1: The values of inhibition efficiency obtained from the weight loss for HA at different concentration in 0.1 M HCl and at different temperatures.**

HA Conc (M)	Temp. (°K)	CR ( $\text{mg}\cdot\text{cm}^{-2}\cdot\text{h}^{-1}$ )	IE (%)	$\theta$
0	298	2.3148	0	0
	303	3.1093	0	0
	308	4.6417	0	0
0.01	298	0.4759	79.44	0.7944
	303	0.7907	76.80	0.7680
	308	1.0222	77.97	0.7797
0.015	298	0.3726	83.90	0.8390
	303	0.4740	86.09	0.8609
	308	0.7425	84.00	0.8400
0.02	298	0.2851	87.68	0.8768
	303	0.3592	89.46	0.8946
	308	0.5259	88.66	0.8866
0.025	298	0.1703	92.64	0.9264
	303	0.2444	92.82	0.9282
	308	0.3000	93.53	0.9353

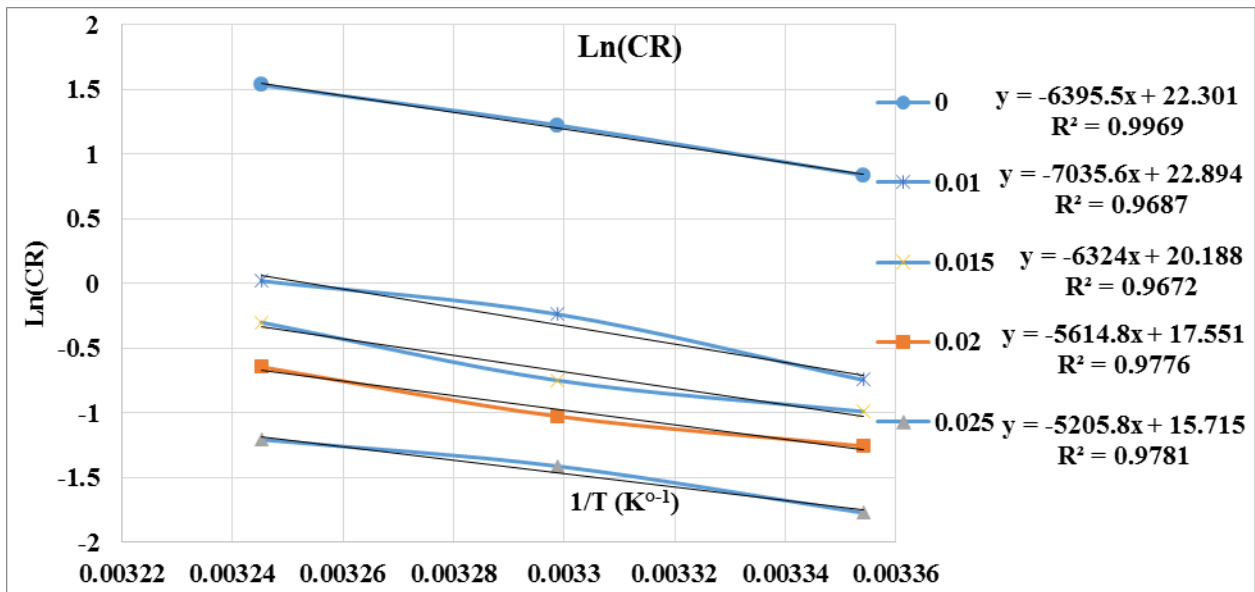


Fig.1: Arrhenius plots of carbon steel in acid with and without different concentrations of HA.

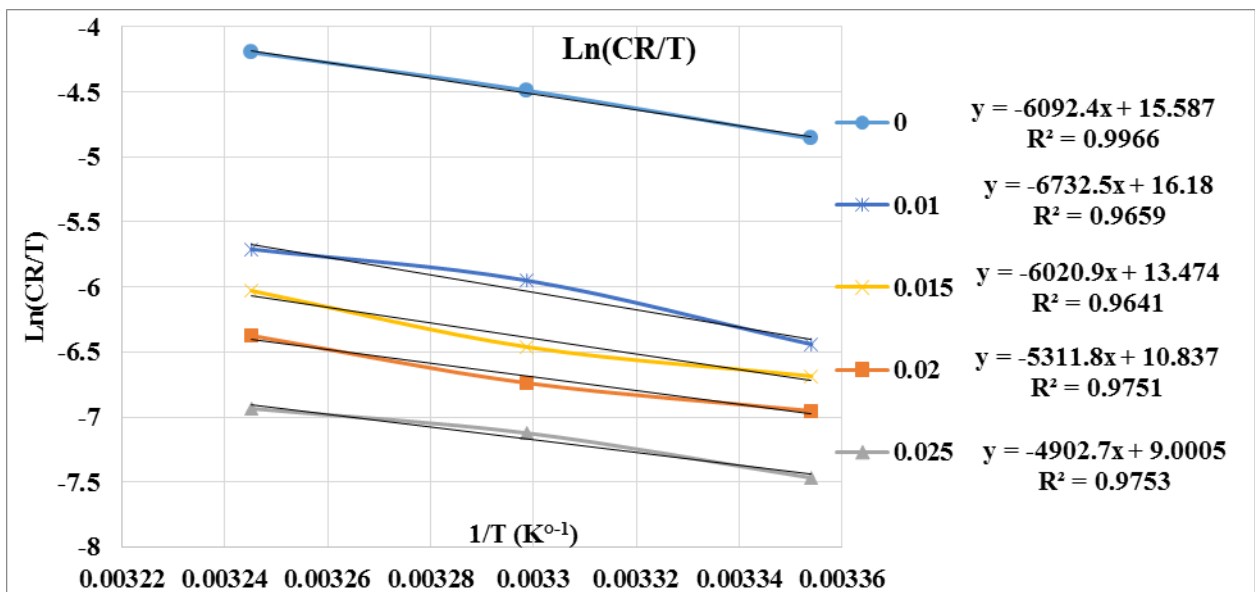


Fig.2: Transition-state plots for carbon steel corrosion rates Ln(CR/T) versus 1/T in 0.1 M HCl in absence and in presence of different concentrations of HA.

The values of activation energy were obtained from the slopes of the linear plots and are given in Table 2. These values indicate that the presence of HA increases the activation energy of the metal dissolution reaction. The adsorption of the inhibitor is assumed to occur on the higher energy sites and the presence of the inhibitor, which results in the blocking of the active sites, must be associated with an increase in the activation energy of carbon steel corrosion in the inhibited state.<sup>[22]</sup> The higher value of  $E_a$  in the presence of HA compared to that in its absence and the decrease in the IE (%) with rise in temperature is interpreted as an indication of physisorption.<sup>[22-24]</sup>

As a result, the increase of HA concentration leads to an increase in the value of  $E_a$ , indicating strong adsorption of the inhibitor molecules at the metal surface.

Table 2: Activation parameters of the dissolution of carbon steel in 0.1 M HCl in the absence and presence of different concentrations of HA.

Conc. (M)	$E_a$ (kJ/mol)	$\Delta H_a$ (kJ/mol)	$\Delta S_a$ (J/mol K)	$E_a - \Delta H_a$ (kJ/mol)
0	53.17	50.65	-67.95	2.519
0.01	58.49	55.97	-63.02	2.519
0.015	52.57	50.05	-85.52	2.519
0.02	46.68	44.16	-107.44	2.519
0.025	43.28	40.76	-122.71	2.519

Examination of these data reveals that the  $\Delta H_a$  values for dissolution reaction of carbon steel in 0.1 M HCl in the presence of HA are higher than that in the absence of HA. The positive sign of  $\Delta H_a$  show the endothermic nature of the solution process suggesting that the

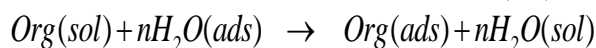
dissolution of carbon steel is slow, which indicates that inhibition efficiencies decrease with increase in temperature. From Table 2, it is seen that the value of activation energy and enthalpy of activation varied in the same way. This result verified the known thermodynamic relation between  $E_a$  and  $\Delta H_a$ .<sup>[25, 26]</sup>

$$E - \Delta H = RT \quad (6)$$

The large negative value of  $\Delta S_a$  for carbon steel in 0.1 M HCl implies that the activated complex is the rate-determining step, rather than the dissociation step. In the presence of the inhibitor, the values of  $\Delta S_a$  increases and is generally interpreted as an increase in disorder as the reactants are converted to the activated complexes.

### 3.2. Adsorption isotherm and thermodynamic consideration

Adsorption isotherms provide information about the interaction of the adsorbed molecules with the metal surface. The adsorption of organic compounds can be expressed by two main types of interactions: physical adsorption and chemical adsorption. There are some factors that influence the adsorption processes including the nature and charge of metal, the chemical of inhibitor, and the type of electrolyte.<sup>[27]</sup> The adsorption of an organic adsorbate at metal-solution interface can be presented as a substitution adsorption process between the organic molecules in aqueous solution,  $Org(sol)$ , and the water molecules on metallic surface,  $H_2O(ads)$ .<sup>[28]</sup>



where  $Org(sol)$  and  $Org(ads)$  are the organic specie dissolved in the aqueous solution and adsorbed onto the metallic surface, respectively,  $H_2O(ads)$  is the water molecule adsorbed on the metallic surface and  $n$  is the size ratio representing the number of water molecules replaced by one organic adsorbate. For the studied inhibitor, it was found that the experimental data obtained from polarization readings could be fitted by Langmuir's adsorption isotherm. According to this isotherm, the surface coverage  $\theta$  is related to inhibitor concentration by.<sup>[29, 30]</sup>

$$\frac{C_{inh}}{\theta} = \frac{1}{K_{ads}} + C_{inh} \quad (7)$$

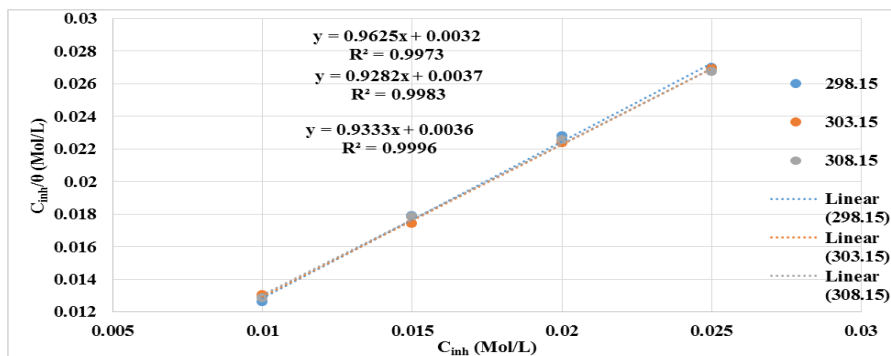


Fig.3. Langmuir's isotherm adsorption model of HA on the carbon steel surface in 0.1 M HCl at different temperatures.

where  $C_{inh}$  denotes the inhibitor concentration,  $\theta$  represents the surface coverage, and  $K_{ads}$  is the equilibrium constant for the adsorption process. Linear plots of  $C_{inh}/\theta$  versus  $C_{inh}$  (Figure 3) yielded regression coefficients ( $R^2$ ) approaching unity and slopes approximating unity, confirming that HA adsorption conforms to the Langmuir model and proceeds via monolayer coverage without significant lateral interactions between adsorbed molecules.<sup>[31]</sup>

The adsorption equilibrium constant  $K_{ads}$ , calculated from the intercepts of Figure 3, decreases with increasing temperature (Table 3), indicating reduced adsorption affinity at elevated temperatures—a trend consistent with exothermic adsorption processes or the thermal destabilisation of physisorbed layers.<sup>[17,18]</sup> The standard Gibbs free energy of adsorption ( $\Delta G_{ads}^\circ$ ) was determined using./

$$K_{ads} = \frac{1}{55.5} \text{Exp}\left(\frac{-\Delta G_{ads}^\circ}{RT}\right) \quad (8)$$

where  $55.5 \text{ mol}\cdot\text{L}^{-1}$  represents the molar concentration of water. The calculated  $\Delta G_{ads}^\circ$  values ( $-24.20$  to  $-24.64 \text{ kJ}\cdot\text{mol}^{-1}$ ; Table 3) fall within the range characteristic of mixed physisorption–chemisorption mechanisms.<sup>[32]</sup> Values more negative than  $-20 \text{ kJ}\cdot\text{mol}^{-1}$  typically indicate electrostatic interactions between charged inhibitor molecules and the metal surface (physisorption), whereas values exceeding  $-40 \text{ kJ}\cdot\text{mol}^{-1}$  suggest charge transfer and coordinate bond formation (chemisorption).<sup>[33,34]</sup> The intermediate magnitude observed herein implies that HA adsorption involves both electrostatic attraction of the protonated amine moiety to the negatively charged steel surface and weak coordinate bonding via the lone pair electrons of the nitrogen atom.<sup>[35]</sup>

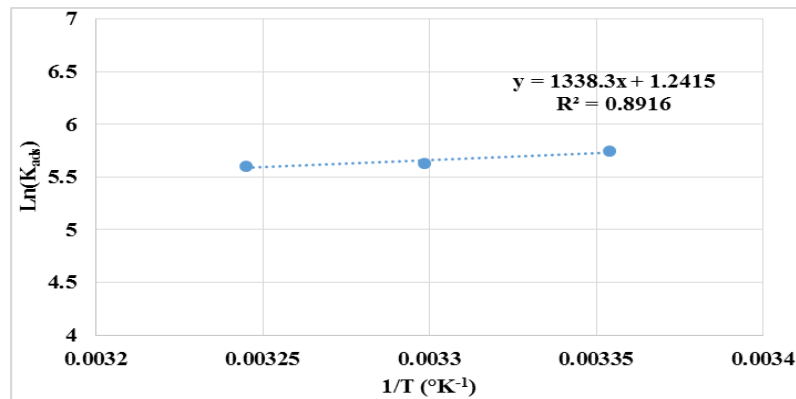
The enthalpy ( $\Delta H_{ads}^\circ$ ) and entropy ( $\Delta S_{ads}^\circ$ ) of adsorption were derived from the van't Hoff relationship.

$$\Delta G_{ads}^\circ = \Delta H_{ads}^\circ - T\Delta S_{ads}^\circ \quad (9)$$

$$\text{Ln}K_{ads} = -\frac{\Delta H_{ads}^\circ}{RT} + \frac{\Delta S_{ads}^\circ}{R} - \text{Ln}(55.5) \quad (10)$$

**Table 3: The thermodynamic parameters of adsorption of HA on the carbon steel surface.**

T (°K)	K <sub>ads</sub> (L/Mol)	$\Delta G_{ads}^{\circ}$ (KJ/Mol)	$\Delta H_{ads}^{\circ}$ (kJ/mol)	$\Delta S_{ads}^{\circ}$ (J/mol)
298	312.50	-24.1957	-11.1266	43.7140
303	277.77	-24.3046		
308	270.27	-24.6353		

**Fig. 4: The relationship between Ln (K<sub>ads</sub>) and 1/T for HA.**

Linear regression of  $\ln(K_{ads})$  versus  $1/T$  (Figure 4) afforded  $\Delta H_{ads}^{\circ} = -11.13 \text{ kJ}\cdot\text{mol}^{-1}$  and  $\Delta S_{ads}^{\circ} = +43.71 \text{ J}\cdot\text{mol}^{-1}\cdot\text{K}^{-1}$  (Table 3). The negative  $\Delta H_{ads}^{\circ}$  value confirms that the adsorption process is exothermic, a characteristic often associated with physisorption.<sup>[25,26]</sup>

The positive  $\Delta S_{ads}^{\circ}$  value reflects an increase in system disorder upon adsorption, which appears counterintuitive given that molecular adsorption typically reduces configurational freedom. This phenomenon is rationalised by the quasi-substitution mechanism, wherein a single HA molecule displaces multiple pre-adsorbed water molecules from the steel surface.<sup>[29,30]</sup> The net increase in the number of free solvent molecules in the bulk phase results in a positive entropy change that outweighs the entropy loss associated with inhibitor immobilization.<sup>[31,32]</sup> This interpretation is consistent with the molecular architecture of HA, wherein the hydrophobic hexyl chain enhances the entropic driving force for adsorption through the hydrophobic effect.<sup>[33,34]</sup>

Collectively, the thermodynamic parameters indicate that HA adsorption on carbon steel in 0.1 M HCl proceeds via a mixed mechanism dominated by electrostatic interactions but supplemented by weak coordinate bonding. The endothermic nature of adsorption, coupled with the positive entropy change, underscores the critical role of solvent reorganisation in governing interfacial inhibitor behavior.<sup>[35,36]</sup>

#### 4. CONCLUSION

Gravimetric investigations confirm that hexylamine functions as a highly effective corrosion inhibitor for carbon steel in 0.1 M hydrochloric acid, achieving a maximum inhibition efficiency of 94.9% at 0.025 M and 298 K, with performance exhibiting positive concentration dependence and marginal thermal

sensitivity attributable to reversible desorption of the adsorbed film. The adsorption process conforms rigorously to the Langmuir isotherm across the investigated temperature range, indicating monolayer coverage without significant lateral interactions between adsorbed species. Kinetic analysis reveals that the presence of hexylamine elevates both the apparent activation energy ( $E_a$ ) and enthalpy of activation ( $\Delta H_a$ ), corroborating the formation of an interfacial energy barrier that impedes anodic metal dissolution. Thermodynamic evaluation yields standard Gibbs free energy of adsorption ( $\Delta G_{ad}^{\circ}$ ) values between  $-24.20$  and  $-24.64 \text{ kJ}\cdot\text{mol}^{-1}$ , signifying a spontaneous process governed by a mixed physisorption–chemisorption mechanism, while the enthalpy ( $\Delta H_{ad}^{\circ} = +11.13 \text{ kJ}\cdot\text{mol}^{-1}$ ) and entropy ( $\Delta S_{ad}^{\circ} = +43.71 \text{ J}\cdot\text{mol}^{-1}\cdot\text{K}^{-1}$ ) of adsorption are mechanistically rationalized through a quasi-substitution model wherein displacement of multiple pre-adsorbed water molecules by a single hexylamine molecule enhances interfacial disorder. Collectively, these findings establish hexylamine as a thermodynamically stable, molecularly efficient inhibitor with significant potential for mitigating acid-induced corrosion in industrial pickling and cleaning applications.

#### 5. REFERENCES

1. Al-Qudsi SS. Arab Demography and Health Provision, Genetic Disorders Among Arab Populations. Springer, 2010; 37–63.
2. Verma C, Olasunkanmi L, Ebenso EE, Quraishi M. Substituents effect on corrosion inhibition performance of organic compounds in aggressive ionic solutions: a review. J Mol Liq., 2018; 251: 100–118.
3. Dariva CG, Galio AF. Corrosion inhibitors—principles, mechanisms and applications. Dev Corros Prot., 2014; 16: 365–378.

4. Goyal M, Kumar S, Bahadur I, et al. Organic corrosion inhibitors for industrial cleaning of ferrous and non-ferrous metals in acidic solutions: a review. *J Mol Liq.*, 2018; 256: 565–573.
5. Arthur DE, Jonathan A, Ameh PO, Anya C. A review on the assessment of polymeric materials used as corrosion inhibitor of metals and alloys. *Int J Ind Chem.*, 2013; 4: 2.
6. Bentiss F, Lebrini M, Lagrenée M. Thermodynamic characterization of metal dissolution and inhibitor adsorption processes in mild steel/2,5-bis(n-thienyl)-1,3,4-thiadiazoles/hydrochloric acid system. *Corros Sci.*, 2005; 47: 2915–2931.
7. Ahamad I, Prasad R, Quraishi M. Experimental and quantum chemical characterization of the adsorption of some Schiff base compounds of phthaloyl thiocarbonylhydrazide on the mild steel in acid solutions. *Mater Chem Phys.*, 2010; 124: 1155–1165.
8. Ebenso E, Ekpe U, Ita B, et al. Effect of molecular structure on the efficiency of amides and thiosemicarbazones used for corrosion inhibition of mild steel in hydrochloric acid. *Mater Chem Phys*, 1999; 60: 79–90.
9. Muralidharan S, Quraishi M, Iyer S. The effect of molecular structure on hydrogen permeation and the corrosion inhibition of mild steel in acidic solutions. *Corros Sci*, 1995; 37: 1739–1750.
10. Braun RD, Lopez EE, Vollmer DP. Low molecular weight straight-chain amines as corrosion inhibitors. *Corros Sci*, 1993; 34: 1251–1257.
11. Khaled K, Babić-Samarđžija K, Hackerman N. Theoretical study of the structural effects of polymethylene amines on corrosion inhibition of iron in acid solutions. *Electrochim Acta.*, 2005; 50: 2515–2520.
12. De Damborenea J, Bastidas J, Vazquez A. Adsorption and inhibitive properties of four primary aliphatic amines on mild steel in 2 M hydrochloric acid. *Electrochim Acta*, 1997; 42: 455–459.
13. Yurt A, Bereket Gz. Combined electrochemical and quantum chemical study of some diamine derivatives as corrosion inhibitors for copper. *Ind Eng Chem Res.*, 2011; 50: 8073–8079.
14. Yin ZF, Feng Y, Zhao W, et al. Effect of temperature on CO<sub>2</sub> corrosion of carbon steel. *Surf Interface Anal.*, 2009; 41: 517–523.
15. Xiang Y, Wang Z, Li Z, Ni W. Effect of temperature on corrosion behaviour of X70 steel in high pressure CO<sub>2</sub>/SO<sub>2</sub>/O<sub>2</sub>/H<sub>2</sub>O environments. *Corros Eng Sci Technol.*, 2013; 48: 121–129.
16. Herrag L, Bouklah M, Patel N, et al. Experimental and theoretical study for corrosion inhibition of mild steel in 1 M HCl solution by some new diaminopropanenitrile compounds. *Res Chem Intermed.*, 2012; 38: 1669–1690.
17. Verma C, Quraishi M, Singh A. 2-Amino-5-nitro-4,6-diarylcyclohex-1-ene-1,3,3-tricarbonitriles as new and effective corrosion inhibitors for mild steel in 1 M HCl: experimental and theoretical studies. *J Mol Liq.*, 2015; 212: 804–812.
18. Fouda AS, El-Aal AA, Kandil AB. The effect of some phthalimide derivatives on corrosion behavior of copper in nitric acid. *Desalination*, 2006; 201: 216–223.
19. Umoren SA, Obot IB, Ebenso EE. Corrosion Inhibition of Aluminium Using Exudate Gum from *Pachylobus edulis* in the Presence of Halide Ions in HCl. *E-Journal Chem*, 2008; 5: 355–364.
20. Umoren SA, Ebenso EE. The synergistic effect of polyacrylamide and iodide ions on the corrosion inhibition of mild steel in H<sub>2</sub>SO<sub>4</sub>. *Mater Chem Phys*, 2007; 106: 387–393.
21. Zarrouk A, Hammouti B, Zarrok H, et al. Thermodynamic study of metal corrosion and inhibitor adsorption processes in copper/N-1-naphthylethylenediamine dihydrochloride monomethanolate/nitric acid system: part 2. *Res Chem Intermed*, 2012; 38: 1655–1668.
22. Zarrouk A, Hammouti B, Zarrok H, et al. Temperature Effect, Activation Energies and Thermodynamic Adsorption Studies of L-Cysteine Methyl Ester Hydrochloride As Copper Corrosion Inhibitor In Nitric Acid 2M. *Int J Electrochem Sci*, 2011; 6: 6261–6274.
23. Badr GE. The role of some thiosemicarbazide derivatives as corrosion inhibitors for C-steel in acidic media. *Corros Sci*, 2009; 51: 2529–2536.
24. Negm NA, Elkholy YM, Zahran MK, et al. Corrosion inhibition efficiency and surface activity of benzothiazol-3-ium cationic Schiff base derivatives in hydrochloric acid. *Corros Sci*, 2010; 52: 3523–3536.
25. Bayol E, Gürten T, Gürten AA, et al. Interactions of some Schiff base compounds with mild steel surface in hydrochloric acid solution. *Mater Chem Phys*, 2008; 112: 624–630.
26. Keleş H. Electrochemical and thermodynamic studies to evaluate inhibition effect of 2-(4-phenoxyphenylimino)methyl]-phenol in 1M HCl on mild steel. *Mater Chem Phys*, 2011; 130: 1317–1324.
27. Amin MA, Mohsen Q, Hazzazi OA. Synergistic effect of I<sup>-</sup> ions on the corrosion inhibition of Al in 1.0M phosphoric acid solutions by purine. *Mater Chem Phys*, 2009; 114: 908–914.
28. Umoren SA, Obot IB, Ebenso EE, et al. The Inhibition of aluminium corrosion in hydrochloric acid solution by exudate gum from *Raphia hookeri*. *Desalination*, 2009; 247: 561–572.
29. Yurt A, Balaban A, Kandemir SU, et al. Investigation on some Schiff bases as HCl corrosion inhibitors for carbon steel. *Mater Chem Phys*, 2004; 85: 420–426.
30. Li X, Deng S, Fu H, et al. Adsorption and inhibition effect of 6-benzylaminopurine on cold rolled steel in 1.0M HCl. *Electrochim Acta*, 2009; 54: 4089–4098.
31. Badiea AM, Mohana KN. Effect of temperature and fluid velocity on corrosion mechanism of low carbon steel in presence of 2-hydrazino-4,7-

- dimethylbenzothiazole in industrial water medium. *Corros Sci*, 2009; 51: 2231–2241.
32. Branzoi V, Branzoi F, Baibarac M. The inhibition of the corrosion of Armco iron in HCl solutions in the presence of surfactants of the type of N-alkyl quaternary ammonium salts. *Mater Chem Phys*, 2000; 65: 288–297.
  33. Keleş H, Keleş M, Dehri İ, et al. The inhibitive effect of 6-amino-m-cresol and its Schiff base on the corrosion of mild steel in 0.5M HCl medium. *Mater Chem Phys*, 2008; 112: 173–179.